Supplementary information of "Structural health monitoring based on a physical reservoir with frequency virtual nodes"

Konosuke Takashima[1], Motoaki Hiraga[2], Nanako Miura[2], and Arata Masuda[2,*]

[1]Division of Mechanophysics, Kyoto Institute of Technology, Kyoto, 606-8585, Japan
[2]Faculty of Mechanical Engineering, Kyoto Institute of Technology, Kyoto, 606-8585, Japan
[*]masuda@kit.ac.jp

ABSTRACT

In this document, detailed information of the responses of the virtual nodes is provided for a further understanding of the behavior of the virtual nodes.

Responses of virtual nodes

In order to understand how the gains and other parameters affect the damage detection accuracy, the responses of the virtual nodes were closely investigated. As described in the main body of the paper, the default values of the parameters were set as follows: common gain $\gamma = 0.1$, feedback gain $G_{\mathrm{fb}} = 1$, virtual node bandwidth $f_w = 20$ Hz, center frequency spacing between adjacent virtual nodes $\Delta f = 10$ Hz, and number of virtual nodes $N = 100$.

Figures S1(a) and (b) show the absolute values of the temporal responses of all virtual nodes $z_i(t)$ $(i = 1, \ldots, N)$ from $t = 20$ to 20.1, when the parameters were set to their default values. This is the case where the damage detection accuracy is favorable, as displayed by the dark blue region in Figs. 7 (a) and (b). The first thing that can be seen from the figures is that some of virtual nodes have very large amplitudes, while the others have relatively small ones. As can be seen from the comparison of Figs. S1(a) and (b), the amplitude distribution of the virtual nodes varies greatly depending on the state of the structure. Looking more closely, the responses of the virtual nodes with large amplitudes show very regular and periodic responses with amplitudes reaching almost one, even though the entire network is driven by white noise. This means that these nodes exhibit limit-cycle responses, suggesting that destabilization of the network by the feedback and amplitude suppression by the saturating nonlinear function tanh are working simultaneously. Notably, such responses are localized at a few nodes, and their distribution differs between the intact and damaged states of the structure, relying on the frequency response function $H_{\mathrm{st}}(\omega)$. This diversity in amplitude ranges is what provides the stable damage detection performance of the network as seen in Figs. 5 (a) and (b), or in other words, what contributes to the "rich" expressiveness of the proposed physical reservoir.

Next, Fig. S2 (a) shows the responses when the common gain is $\gamma = 10^{-4}$ and the feedback gain is $G_{\mathrm{fb}} = 10^{-2}$, with the structure in the intact state. This set of parameters corresponds to the lower left corner of Figs. 7(a) and (b) belonging to the light blue region. As shown in Fig. S2 (a), the waveform becomes random with very small (in the order of 10^{-3}) amplitude. This is because the system becomes asymptotically stable since the loop gain is extremely small (10^{-6}). Consequently, the node responses lose diversity and regularity, which leads to the low damage detection accuracy. Conversely, Fig. S2 (b) shows the responses when the common gain is $\gamma = 10^{2}$ and the feedback gain is $G_{\mathrm{fb}} = 10^{4}$, with the structure in the intact state. This set of parameters corresponds to the upper right corner of Figs. 7(a) and (b) belonging to the yellow region. As shown in Fig. S2 (b), every node responds in a square wave with an amplitude of one. This indicates that all the virtual nodes exhibit limit-cycles with unit amplitude because of the extremely high loop gain (10^{6}). This time, the node responses are regular but lack any diversity, again losing the characteristics required of the physical reservoir. This is the reason for the worst damage detection accuracy observed in Figs. 7(a) and (b).

Finally, the responses of the virtual nodes for altered bandwidth were investigated. Figure S3 (a) shows the responses when the bandwidth is $f_w = 5$ Hz with the structure in the intact state. As shown in Fig. S3 (a), most nodes respond in a square wave with an amplitude of one except for some nodes responding in smaller amplitude. Meanwhile, Fig. S3 (b) shows the responses when the bandwidth is $f_w = 70$ Hz with the structure in the intact state. In this case, the performance index is the RMSE $E_{rms} = 0.7229$. Figure S3 (b) indicates that, while the low frequency nodes respond in a square wave with an amplitude of one, more than half of the nodes exhibit significant amplitude modulation. This makes the node responses lose diversity and temporal stationarity, which leads to the low damage detection accuracy.

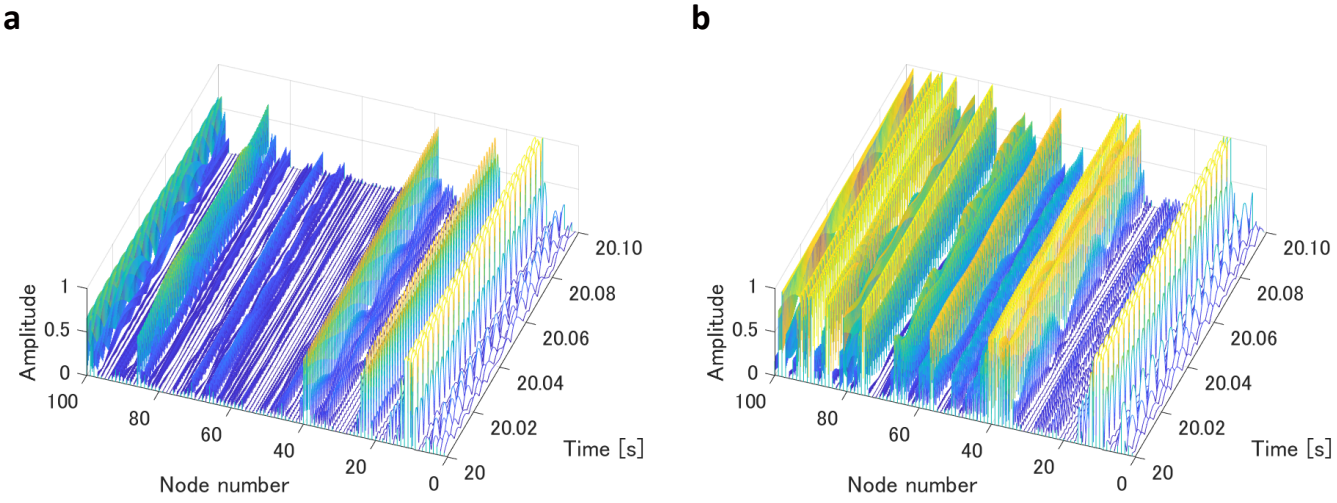

Figure S1. The absolute values of the temporal responses of all virtual nodes $z_i(t)$ $(i = 1, \ldots, N)$ from $t = 20$ to 20.1, when the parameters were set to the default values. (**a**) Responses of all virtual nodes , when the structure is in the intact state. (**b**) Responses of all virtual nodes, when the structure is in the damaged state.

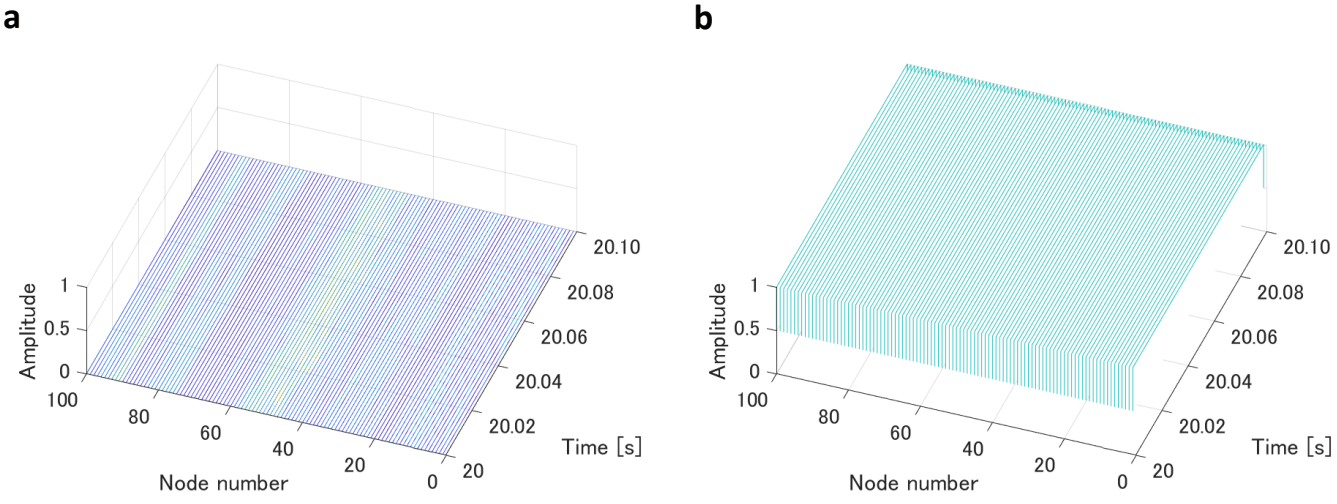

Figure S2. The absolute values of the temporal responses of all virtual nodes $z_i(t)$ $(i = 1, \ldots, N)$ from $t = 20$ to 20.1, when the structure is in the intact state. (**a**) Responses of all virtual nodes when the common gain is $\gamma = 10^{-4}$ and the feedback gain is $G_{\mathrm{fb}} = 10^{-2}$, corresponding to the light blue region in Figs. 7(a) and (b). (**b**) Responses of all virtual nodes when the common gain is $\gamma = 10^{2}$ and the feedback gain is $G_{\mathrm{fb}} = 10^{4}$, corresponding to the yellow region in Figs. 7(a) and (b)

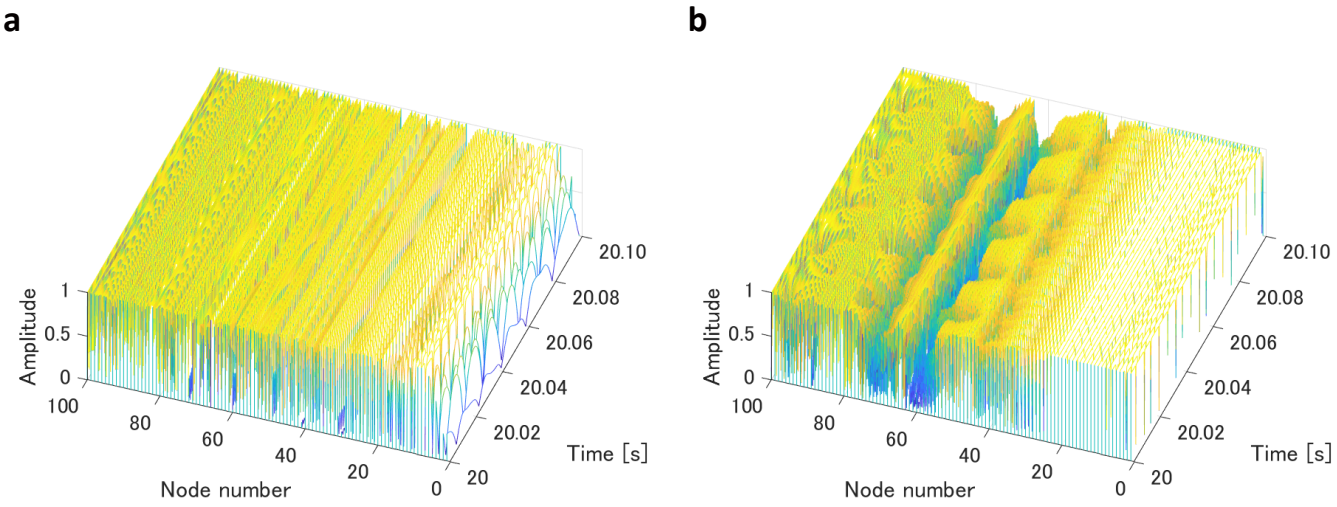

Figure S3. The absolute values of the temporal responses of all virtual nodes $z_i(t)$ $(i = 1, \ldots, N)$ from $t = 20$ to 20.1, when the structure is in the intact state. (**a**) Responses of all virtual nodes when the virtual node bandwidth is $f_w = 5$ Hz. (**b**) Responses of all virtual nodes when the virtual node bandwidth is $f_w = 70$ Hz.